

Nutation in antiferromagnetic resonance

Ritwik Mondal,^{*} Sebastian Großenbach, Levente Rózsa, and Ulrich Nowak

Fachbereich Physik, Universität Konstanz, DE-78457 Konstanz, Germany

(Dated: July 19, 2022)

The effect of inertial spin dynamics is compared between ferromagnetic, antiferromagnetic and ferrimagnetic systems. The linear response to an oscillating external magnetic field is calculated within the framework of the inertial Landau–Lifshitz–Gilbert equation using analytical theory and computer simulations. Precession and nutation resonance peaks are identified, and it is demonstrated that the precession frequencies are reduced by the spin inertia, while the lifetime of the excitations is enhanced. The interplay between precession and nutation is found to be the most prominent in antiferromagnets, where the timescale of the exchange-driven sublattice dynamics is comparable to inertial relaxation times. Consequently, antiferromagnetic resonance techniques should be better suited for the search for intrinsic inertial spin dynamics on ultrafast timescales than ferromagnetic resonance.

Deterministic spin switching at ultrashort timescales builds the fundament for future spin-based memory technology [1–5]. At femtosecond timescales inertial switching becomes particularly relevant, where the reversal is achieved with a linear momentum gained by the interaction of an ultrashort pulse and spin inertia [6, 7]. The understanding of magnetic inertia has been pursued along two different directions so far.

On the one hand, spin dynamics in antiferromagnets (AFMs) and ferrimagnets (FiMs) has successfully been described by the Landau–Lifshitz–Gilbert (LLG) equation [8–10] for two sublattices coupled by the exchange interaction. The exchange energy created by tilting the sublattice magnetization directions away from the antiferromagnetic orientation is dynamically transformed into anisotropy energy by collectively rotating the sublattices away from the easy magnetic direction [11], analogously to the transition between kinetic and potential energy terms in a harmonic oscillator. While the LLG equation for the two sublattices is of first order in time, this effect gives rise to an effectively inertial second-order differential equation for the order parameter in AFMs [12, 13]. The interaction between exchange and anisotropy degrees of freedom causes an exchange enhancement of AFM resonance frequencies and linewidths [14].

On the other hand, an intrinsic inertia also arises in magnetic systems, if it is assumed that the directions of spin angular and magnetic moments become separated in the ultrafast dynamical regime [15, 16]. The inertia gives rise to spin nutation, a rotation of the magnetization around the angular momentum direction [17], caused by the energy transfer between magnetic kinetic and potential energy terms. The emergence of spin inertia has been explained based on an extension of the breathing Fermi surface model [18, 19], calculated from a $s-d$ like interaction between the magnetization density and electron spin [20] and derived from a fundamental relativistic Dirac theory [21, 22]. Magnetic inertia can be associated with a torque term containing a second-order time derivative of the magnetic moment appearing in the inertial LLG (ILLG) dynamical equation. The characteristic inertial relaxation time is expected to range from 1 fs [15, 20, 23, 24] to a few hundred fs [25].

Linear-response theory predicted the emergence of a nu-

tation resonance besides the conventional precession resonance in ferromagnets (FMs) [26–28], providing a possible way of detecting inertial dynamics by applying oscillating external fields. An indirect evidence of the inertial dynamics was found in NiFe and Co samples [23] by following the field dependence of the ferromagnetic precession resonance (FMR) peaks. The experimental observation of the nutation resonance has only been achieved very recently in NiFe and CoFeB using intense terahertz magnetic field transients [25].

While the notion of inertial dynamics has been applied both in the context of the LLG equation for AFMs as well as in the ILLG equation for FMs, the linear response of these two examples is fundamentally different. While in both cases a pair of resonances is found in contrast to the single FMR peak, the excitation frequencies in an AFM are degenerate in the absence of a static external field, while they differ by several orders of magnitude in the ILLG equation. The effective damping parameter of the precession, defined as the half-width of the peak at half-maximum, is considerably higher in AFMs than in FMs, where it corresponds to the Gilbert damping. In contrast, it was demonstrated that the effective damping decreases in the ILLG equation applied to FMs [27], particularly at the nutation resonance [29]. However, the ILLG has not been applied to AFMs so far.

Here, we explore the effects of the ILLG equation in two-sublattice AFMs and FiMs using linear-response theory and computer simulations. It is shown that a pair of nutation resonance peaks emerges, and that the inertial relaxation time influences the precessional resonance significantly stronger in AFMs than in FMs due to the exchange coupling between the sublattices. The effective damping parameter is found to decrease in AFMs, reaching considerably lower values than the Gilbert damping at the nutation peak, thereby enhancing the lifetime of these excitations. The inertial effects in FiMs are found to interpolate between those in AFMs and FMs.

As derived in earlier works [15, 21, 22], the ILLG equation reads

$$\dot{\mathbf{M}}_i = -\gamma_i \mathbf{M}_i \times \mathbf{H}_i + \frac{\alpha_i}{M_{i0}} \mathbf{M}_i \times \dot{\mathbf{M}}_i + \frac{\eta}{M_{i0}} \mathbf{M}_i \times \ddot{\mathbf{M}}_i, \quad (1)$$

generalized here to multiple sublattices indexed by i . The first, second and third terms in Eq. (1) describe spin precession with gyromagnetic ratio γ_i , transverse relaxation with Gilbert damping α_i and inertial dynamics with relaxation time η_i . Note that an alternative notation for the inertial term with $\eta_i = \alpha_i \tau_i$ is also used in the literature [15, 23, 25]; where comparison with earlier works is mentioned in the following, the relaxation time is converted to the formulation of Eq. (1).

First, we summarize the effects of the inertial term on FM resonance. The FM is described by the free energy $\mathcal{F}(\mathbf{M}) = -H_0 M_z - K M_z^2 / M_0^2$, modeling a single sublattice where spatial modulations of the magnetization are neglected. M_0 is the magnitude of the magnetic moment, H_0 is the applied external field and K is the uniaxial anisotropy energy, also considered to include demagnetization effects in the form of a shape anisotropy. The effective field can be written as $\mathbf{H} = -\partial\mathcal{F}/\partial\mathbf{M} = (H_0 + 2KM_z/M_0^2)\hat{\mathbf{e}}_z$, and the magnetic moment is oriented along the z direction in equilibrium.

The linear response to a small transversal external field component $\mathbf{h}(t)$ is calculated considering $\mathbf{M} = M_0\hat{\mathbf{e}}_z + \mathbf{m}(t)$ and expanding Eq. (1) up to first order in $\mathbf{h}(t)$ and $\mathbf{m}(t)$. The exciting field is assumed to be circularly polarized, $h_{\pm} = h_x \pm ih_y = he^{\pm i\omega t}$, with a similar time dependence for the response, $m_{\pm} = m_x \pm im_y = me^{\pm i\omega t}$. The calculated susceptibility reads (see the Supplemental Material [30] for details)

$$m_{\pm} = \chi_{\pm} h_{\pm} = \frac{\gamma M_0}{\Omega_0 - \omega - \eta\omega^2 \pm i\alpha\omega} h_{\pm}, \quad (2)$$

with $\Omega_0 = \gamma(H_0 M_0 + 2K)/M_0$. It is found that the Gilbert damping is associated with the imaginary part of the susceptibility, while the inertial term contributes to the real part of the susceptibility, which is consistent with the previous calculation in Ref. [21]. The dissipated power is calculated as $P = \dot{\mathbf{m}} \cdot \mathbf{h} = \omega \text{Im}(\chi_+) |h|^2$.

The dissipated power with and without the inertial term is shown in Fig. 1. The relaxation time is chosen to be $\eta = 10^{-13}$ s, higher than the fs timescales described in Refs. [20, 23, 24], but somewhat lower than the values of around 300 fs in Ref. [25]. It can be observed that the inertial dynamics reduces the precession resonance frequency. The resonance peak position is well approximated as $\omega_p = (\sqrt{1 + 4\beta_{\text{FM}}} - 1) / (2\eta) \approx \Omega_0(1 - \beta_{\text{FM}})$, with $\beta_{\text{FM}} = \eta\Omega_0$. The associated shift in the resonance field H_p was investigated in Ref. [23]. However, note that the relative value of this shift is very low since $\beta_{\text{FM}} \ll 1$, meaning that it can only be observed if Ω_0 is shifted to high values, for example by a strong external field H_0 .

The most profound effect of the inertial dynamics is the emergence of a second resonance peak, associated with the spin nutation. Its frequency is approximately $\omega_n = -(\sqrt{1 + 4\beta_{\text{FM}}} + 1) / (2\eta) \approx -1/\eta - \Omega_0(1 - \beta_{\text{FM}})$. Similarly to the precession frequency, the subleading corrections $\beta_{\text{FM}}\Omega_0$ are small. The negative sign of the frequency im-

plies an opposite rotational sense [32]: while the precession is excited by a circularly polarized field rotating counter-

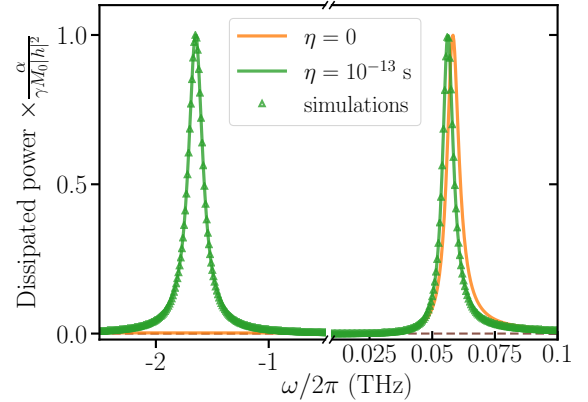


Figure 1. (Color Online) The dissipated power for FMR with and without the inertial term, with $\eta = 10^{-13}$ s in the first case. The lines and symbols represent analytical and simulation results (see the Supplemental Material for details [30]). For the other parameters see [31].

clockwise, the nutation resonance reveals an opposite polarization.

The effective damping parameter is defined as the ratio of the imaginary and the real parts of the frequency where Eq. (2) has a node, and is approximately expressed as $\alpha_{\text{eff,p}} = \alpha_{\text{eff,n}} \approx \alpha(1 - 2\beta_{\text{FM}})$, see the Supplemental Material [30] for the derivation. Since the imaginary part characterizes the half-width of the resonance peak at half maximum, the latter suggests that the linewidth of FMR decreases due to the inertia in agreement with the numerical results in Ref. [27]. The relative value of the reduction is once again governed by the factor β_{FM} .

Next, we consider AFMs and FiMs with two sublattices A and B . Assuming once again homogeneous sublattice magnetizations, the free energy is expressed as

$$\mathcal{F}(\mathbf{M}_A, \mathbf{M}_B) = -H_0(M_{Az} + M_{Bz}) - \frac{K_A}{M_{A0}^2} M_{Az}^2 - \frac{K_B}{M_{B0}^2} M_{Bz}^2 + \frac{J}{M_{A0}M_{B0}} \mathbf{M}_A \cdot \mathbf{M}_B, \quad (3)$$

with the external field applied along the z direction, $\mathbf{H}_0 = H_0\hat{\mathbf{e}}_z$, uniaxial easy-axis anisotropy constants K_A, K_B and intersublattice exchange coupling J . From the free energy, the associated fields entering the sublattice LLG equations (1) can be determined using $\mathbf{H}_{A/B} = -\partial\mathcal{F}(\mathbf{M}_A, \mathbf{M}_B)/\partial\mathbf{M}_{A/B} = H_0\hat{\mathbf{e}}_z + 2K_{A/B}M_{A/Bz}/M_{A/B0}^2\hat{\mathbf{e}}_z - JM_{B/A}/(M_{A0}M_{B0})$. In equilibrium, the sublattice magnetizations are aligned antiparallel along the z direction. Linear response to the transverse homogeneous external field $\mathbf{h}_A(t) = \mathbf{h}_B(t)$ may be calculated similarly to the FM case, using the expansions $\mathbf{M}_A(\mathbf{r}, t) = M_{A0}\hat{\mathbf{e}}_z + \mathbf{m}_A(t)$ and $\mathbf{M}_B(\mathbf{r}, t) = -M_{B0}\hat{\mathbf{e}}_z + \mathbf{m}_B(t)$.

The two-sublattice susceptibility tensor is expressed as follows (see Supplemental Material [30]):

$$\begin{pmatrix} m_{A\pm} \\ m_{B\pm} \end{pmatrix} = \chi_{\pm}^{AB} \begin{pmatrix} h_{A\pm} \\ h_{B\pm} \end{pmatrix} = \frac{1}{\Delta_{\pm}} \begin{pmatrix} \frac{1}{\gamma_B M_{B0}} (\Omega_B \pm i\omega\alpha_B - \eta_B\omega^2 + \omega) & -\frac{1}{M_{A0}M_{B0}} J \\ -\frac{1}{M_{A0}M_{B0}} J & \frac{1}{\gamma_A M_{A0}} (\Omega_A \pm i\omega\alpha_A - \eta_A\omega^2 - \omega) \end{pmatrix} \begin{pmatrix} h_{A\pm} \\ h_{B\pm} \end{pmatrix}, \quad (4)$$

Here we use the definitions $\Delta_{\pm} = (\gamma_A M_{A0} \gamma_B M_{B0})^{-1} (\Omega_A \pm i\omega\alpha_A - \eta_A\omega^2 - \omega) (\Omega_B \pm i\omega\alpha_B - \eta_B\omega^2 + \omega) - J^2 / (M_{A0}^2 M_{B0}^2)$ as well as $\Omega_A = \gamma_A / M_{A0} (J + 2K_A + H_0 M_{A0})$ and $\Omega_B = \gamma_B / M_{B0} (J + 2K_B - H_0 M_{B0})$.

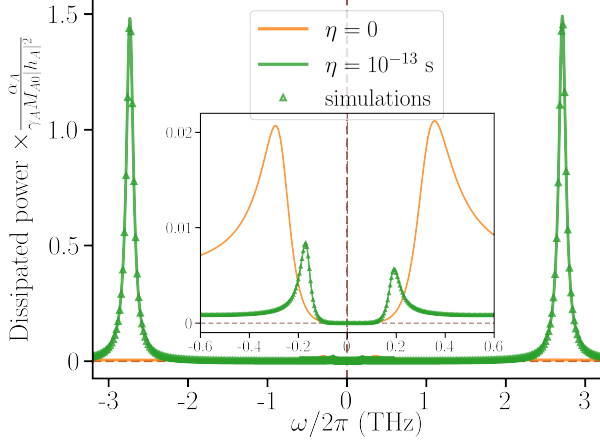


Figure 2. (Color Online) The dissipated power for AFMR with and without the inertial term, with $\eta = \eta_A = \eta_B = 10^{-13}$ s in the former case. The lines and symbols represent analytical and simulation results. The other parameters are given in [33].

To compare with FMR, we compute the dissipated power for AFMR, $P = \dot{\mathbf{m}}_A \cdot \mathbf{h}_A + \dot{\mathbf{m}}_B \cdot \mathbf{h}_B$, with the explicit formula given in the Supplemental Material [30]. The result is shown in Fig. 2, using the same parameters for both sublattices as for the FM in Fig. 1. The inset of Fig. 2 shows that without the inertial term the AFM precession resonance peaks are suppressed with respect to the FM one by a factor of about $J/(2K) = 50$. This is caused by the fact that the magnetization in the two sublattices rotates around the equilibrium direction with a phase shift of π , meaning that the homogeneous exciting field only couples to the difference of the sublattice precession amplitudes [14] in the dissipated power. Also, the inertial term shifts the precession resonance peaks to lower frequencies considerably stronger than in the FM, and further reduces their magnitude. At higher frequency, two additional nutation resonance peaks can be observed. Remarkably, their height is significantly larger than that of the precession resonances, even exceeding the intensity of the FMR peaks (cf. Fig. 1 where the same normalization was used). The latter suggests that probing the AFM nutation resonance peak is experimentally more suitable than in the FM case. Most of these effects can be explained by the fact that the precession and nutation resonance frequencies lie much closer in AFMs than in FMs, as will be discussed in detail below.

To obtain the AFM resonance frequencies, we calculate the nodes of the susceptibility tensor in Eq. (4), obtaining

$$\Delta_{\pm} = a_{\pm}\omega^4 + b_{\pm}\omega^3 + c_{\pm}\omega^2 + d_{\pm}\omega + e_{\pm} = 0. \quad (5)$$

with the following definitions:

$$a_{\pm} = \eta_A \eta_B, \quad (6)$$

$$b_{\pm} = \mp i(\alpha_A \eta_B + \alpha_B \eta_A) - (\eta_A - \eta_B), \quad (7)$$

$$c_{\pm} = -1 \pm i(\alpha_A - \alpha_B) - (\Omega_A \eta_B + \Omega_B \eta_A) - \alpha_A \alpha_B, \quad (8)$$

$$d_{\pm} = (\Omega_A - \Omega_B) \pm i(\alpha_B \Omega_A + \alpha_A \Omega_B), \quad (9)$$

$$e_{\pm} = -\frac{\gamma_A}{M_{A0}} \frac{\gamma_B}{M_{B0}} J^2 + \Omega_A \Omega_B. \quad (10)$$

Note that inertial effects enter via a , b , and c , terms which are of higher order in frequency. Setting the inertial relaxation times to zero, we obtain a second-order equation that results in well-known antiferromagnetic resonance frequencies [34–36]. For equivalent sublattices and assuming $\alpha \ll 1$ and $K \approx H_0 M_0 \ll J$, these read $\omega_{p\pm} \approx \left(1 \pm i\alpha\sqrt{J/(4K)}\right) \left(\gamma H_0 \pm \gamma/M\sqrt{4KJ}\right)$. Compared to the FM case, two resonance frequencies are found, and they are exchange enhanced by about a factor of $\sqrt{J/K}$. However, the lifetime of the excitations is reduced since the effective damping is also higher by a factor of $\sqrt{J/(4K)}$.

In the presence of the inertial term, the resonance frequencies are found as a solution of a fourth-order equation. These have been calculated for an AFM and an FiM as a function of the relaxation time $\eta_A = \eta_B = \eta$ in Fig. 3. In the absence of external field and damping, Eq. (5) simplifies to a second-order equation in ω^2 . The precession resonance frequencies are given by $\omega_{p\pm} \approx \pm \gamma/M\sqrt{4KJ} (1 + 2\beta_{\text{AFM}})^{-\frac{1}{2}}$ for $K \ll J$. It is important to note here that the relative strength of the inertial corrections is defined by the dimensionless parameter $\beta_{\text{AFM}} = \eta\gamma/MJ$, which is enhanced by a factor of J/K as compared to β_{FM} . The characteristic time scale of the exchange interactions typically falls into the fs range in AFMs which are ordered at room temperature ($\gamma/MJ \approx 10^{13} \text{ s}^{-1}$ with the parameters used here), which is similar to the typical values of the inverse inertial relaxation time [20, 23, 25]. This explains the considerable decrease of the AFMR precession frequencies in Fig. 2, while Fig. 3(a) demonstrates that deviations from the non-inertial case already become observable for $\eta \approx 1$ fs. This more pronounced inertial effect should also be observable if the resonance is measured by sweeping the external field, as in Ref. [23]. The strongly asymmetric ($M_{A0} = 5M_{B0}$) FiM in Fig. 3(b) is characterized by a high-frequency exchange mode, strongly influenced by inertial effects as in the AFM, and a low-frequency mode which is less affected like in the FM.

The nutation resonance frequencies in the AFM can be expressed as $\omega_{n\pm} \approx \pm \sqrt{1 + 2\beta_{\text{AFM}}}/\eta$. Just as for the pre-

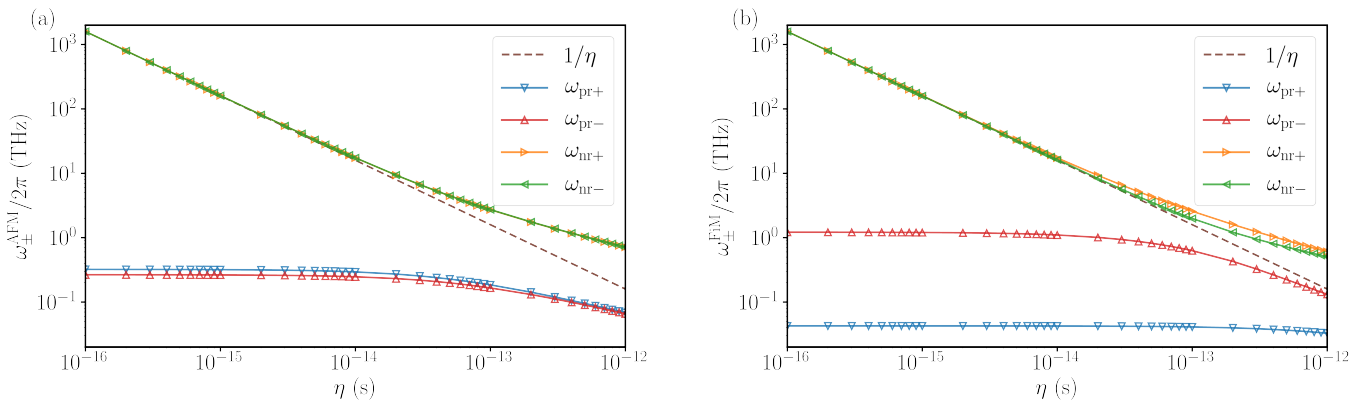


Figure 3. (Color Online) Real part of the precession resonance frequencies as a function of inertial relaxation time η , (a) for AFMs with $M_{A0} = M_{B0} = 2\mu_B$ and (b) for FiMs with $M_{A0} = 5M_{B0} = 10\mu_B$. The other parameters are given in [33].

cession resonance, the correction factor arising due to the interplay between inertia and magnetic interactions is given by β_{AFM} , which is exchange enhanced compared to the FM case. This gives rise to an increase of the nutation frequencies, as demonstrated in Fig. 2. For the FiM in Fig. 3(b), the nutation frequency $\omega_{\text{nr}+}$ belonging to the exchange mode $\omega_{\text{pr}-}$ starts deviating from the low-inertia η^{-1} asymptote at considerably lower frequencies than the FM-like nutation $\omega_{\text{nr}-}$.

The effective damping parameters of the excitation modes, defined as the ratio of the imaginary to the real part of the frequencies, are shown in Fig. 4. They no longer coincide between precession and nutation as in the FM case, since the exchange enhancement discussed above does not affect the nutation resonance. A reduction of the effective damping is observed with increasing inertial relaxation times, which becomes noticeable for $\beta_{\text{AFM}} = O(10^{-2})$, just as in the case of the resonance frequencies. The considerable reduction of the effective damping compared to the Gilbert damping leads to sharper nutation resonance peaks as demonstrated in Fig. 2, with higher intensities than for the FM. In the FiM, the exchange modes $\omega_{\text{n}+}$ and $\omega_{\text{p}-}$ start to become influenced at lower inertial relaxation times than the FM modes $\omega_{\text{n}-}$ and $\omega_{\text{p}+}$ [37]. The difference between the effective damping parameters vanishes between exchange and FM modes for higher η , but it remains to be observable between precession and nutation modes.

To conclude, we applied the ILLG equation to FMs and to two-sublattice AFMs and FiMs, and investigated the resonance frequencies using linear-response theory and computer simulations. The precession frequencies are found to decrease with increasing inertial relaxation time and additional high-frequency nutation peaks become observable. Furthermore, the calculation of the resonance linewidth shows that the effect of inertia reduces the effective damping parameter. While in FMs these corrections scale with $\beta_{\text{FM}} = \eta\Omega_0$, in AFMs the dimensionless coupling between precession and nutation is given by $\beta_{\text{AFM}} = \eta\gamma/MJ$, which is typically several orders of magnitude higher. The FiM is observed to interpolate between the FM and AFM limits. The reduced effective damping gives rise to particu-

larly sharp and high-intensity nutation resonance peaks in AFMs, with frequencies comparable to the values already observed in FMs [23, 25]. These findings are expected to motivate the search for the signs of intrinsically inertial spin dynamics on ultrafast timescales using AFMR techniques.

We acknowledge financial support from the Alexander von Humboldt-Stiftung, the Deutsche Forschungsgemeinschaft via Project No. NO 290/5-1, and the National Research, Development, and Innovation Office of Hungary via Project No. K131938.

* ritwik.mondal@uni-konstanz.de

- [1] C. D. Stanciu, F. Hansteen, A. V. Kimel, A. Kirilyuk, A. Tsukamoto, A. Itoh, and T. Rasing, *Phys. Rev. Lett.* **99**, 047601 (2007).
- [2] K. Vahaplar, A. M. Kalashnikova, A. V. Kimel, D. Hinzke, U. Nowak, R. Chantrell, A. Tsukamoto, A. Itoh, A. Kirilyuk, and T. Rasing, *Phys. Rev. Lett.* **103**, 117201 (2009).
- [3] I. Radu, K. Vahaplar, C. Stamm, T. Kachel, N. Pontius, H. A. Dürr, T. A. Ostler, J. Barker, R. F. L. Evans, R. W. Chantrell, A. Tsukamoto, A. Itoh, A. Kirilyuk, T. Rasing, and A. V. Kimel, *Nature* **472**, 205 (2011).
- [4] K. Vahaplar, A. M. Kalashnikova, A. V. Kimel, S. Gerlach, D. Hinzke, U. Nowak, R. Chantrell, A. Tsukamoto, A. Itoh, A. Kirilyuk, and Th. Rasing, *Phys. Rev. B* **85**, 104402 (2012).
- [5] A. Hassdenteufel, B. Hebler, C. Schubert, A. Liebig, M. Teich, M. Helm, M. Aeschlimann, M. Albrecht, and R. Bratschitsch, *Advanced Materials* **25**, 3122 (2013).
- [6] A. V. Kimel, B. A. Ivanov, R. V. Pisarev, P. A. Usachev, A. Kirilyuk, and Th. Rasing, *Nat. Phys.* **5**, 727 (2009).
- [7] S. Wienholdt, D. Hinzke, and U. Nowak, *Phys. Rev. Lett.* **108**, 247207 (2012).
- [8] L. D. Landau and E. M. Lifshitz, *Phys. Z. Sowjetunion* **8**, 101 (1935).
- [9] T. L. Gilbert and J. M. Kelly, in *American Institute of Electrical Engineers* (New York, October 1955) pp. 253–263.
- [10] T. L. Gilbert, *IEEE Transactions on Magnetics* **40**, 3443 (2004).
- [11] L. Rózsa, S. Selzer, T. Birk, U. Atxitia, and U. Nowak, *Phys. Rev. B* **100**, 064422 (2019).
- [12] E. V. Gomonaï and V. M. Loktev, *Low Temp. Phys.* **34**,

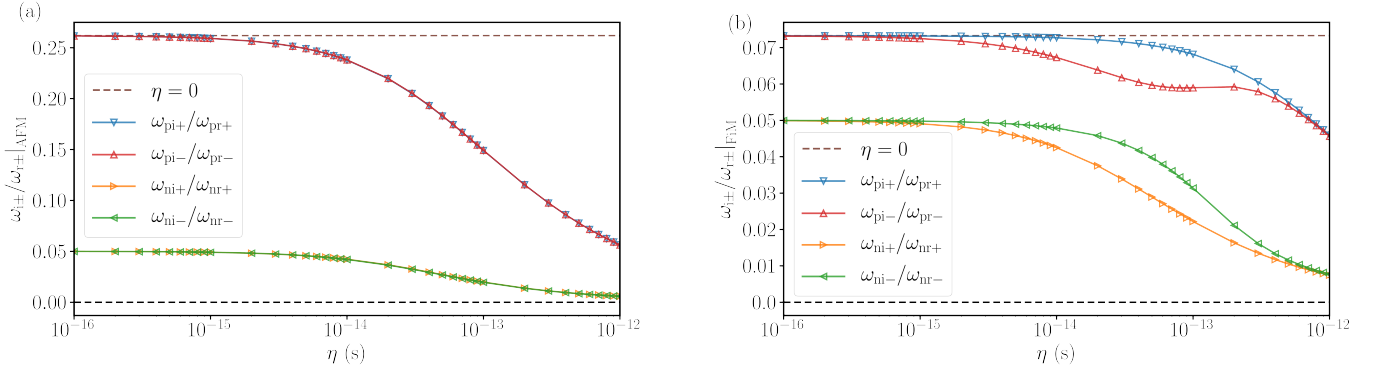


Figure 4. (Color Online) Effective damping parameters of the resonance modes as a function of inertial relaxation time η , for (a) AFMs with $M_{A0} = M_{B0} = 2\mu_B$ and (b) FiMs with $M_{A0} = 5M_{B0} = 10\mu_B$. The other parameters are given in [33].

- 198 (2008).
- [13] K. M. D. Hals, Y. Tserkovnyak, and A. Brataas, *Phys. Rev. Lett.* **106**, 107206 (2011).
- [14] A. G. Gurevich and G. A. Melkov, *Magnetization Oscillations and Waves*, Lecture Notes in Physics (CRC Press, 1996).
- [15] M.-C. Ciornei, J. M. Rubí, and J.-E. Wegrowe, *Phys. Rev. B* **83**, 020410 (2011).
- [16] J.-E. Wegrowe and M.-C. Ciornei, *Am. J. Phys.* **80**, 607 (2012).
- [17] D. Böttcher and J. Henk, *Phys. Rev. B* **86**, 020404 (2012).
- [18] M. Fähnle, D. Steiauf, and C. Illg, *Phys. Rev. B* **84**, 172403 (2011).
- [19] M. Fähnle and C. Illg, *J. Phys.: Condens. Matter* **23**, 493201 (2011).
- [20] S. Bhattacharjee, L. Nordström, and J. Fransson, *Phys. Rev. Lett.* **108**, 057204 (2012).
- [21] R. Mondal, M. Berritta, A. K. Nandy, and P. M. Oppeneer, *Phys. Rev. B* **96**, 024425 (2017).
- [22] R. Mondal, M. Berritta, and P. M. Oppeneer, *J. Phys.: Condens. Matter* **30**, 265801 (2018).
- [23] Y. Li, A.-L. Barra, S. Auffret, U. Ebels, and W. E. Bailey, *Phys. Rev. B* **92**, 140413 (2015).
- [24] D. Thonig, O. Eriksson, and M. Pereiro, *Sci. Rep.* **7**, 931 (2017).
- [25] K. Neeraj, N. Awari, S. Kovalev, D. Polley, N. Zhou Hagström, S. S. P. K. Arekapudi, A. Semisalova, K. Lenz, B. Green, J.-C. Deinert, I. Ilyakov, M. Chen, M. Bawatna, V. Scalera, M. d’Aquino, C. Serpico, O. Hellwig, J.-E. Wegrowe, M. Gensch, and S. Bonetti, *Nat. Phys.* (2020), <https://doi.org/10.1038/s41567-020-01040-y>.
- [26] E. Olive, Y. Lansac, and J.-E. Wegrowe, *Appl. Phys. Lett.* **100**, 192407 (2012).
- [27] E. Olive, Y. Lansac, M. Meyer, M. Hayoun, and J.-E. Wegrowe, *J. Appl. Phys.* **117**, 213904 (2015).
- [28] M. Cherkasskii, M. Farle, and A. Semisalova, “Nutation resonance in ferromagnets,” (2020), [arXiv:2008.12221 \[cond-mat.mes-hall\]](https://arxiv.org/abs/2008.12221).
- [29] I. Makhfudz, E. Olive, and S. Nicolis, *Appl. Phys. Lett.* **117**, 132403 (2020).
- [30] See Supplementary Material for details of the atomistic simulations and the derivation of the susceptibility, the dissipated power, the resonance frequencies and the effective damping parameters.
- [31] The following parameters are used for the FM: $\gamma = 1.76 \times 10^{11} \text{ T}^{-1}\text{s}^{-1}$, $K = 10^{-23} \text{ J}$, $M_0 = 2\mu_B$, $\alpha = 0.05$, $H_0 = 1 \text{ T}$ and $|h| = 0.001 \text{ T}$.
- [32] T. Kikuchi and G. Tatara, *Phys. Rev. B* **92**, 184410 (2015).
- [33] The following parameters are used for the AFM and the FiM: $\gamma_A = \gamma_B = \gamma = 1.76 \times 10^{11} \text{ T}^{-1}\text{s}^{-1}$, $J = 10^{-21} \text{ J}$, $K_A = K_B = K = 10^{-23} \text{ J}$, $M_{B0} = 2\mu_B$, $\alpha_A = \alpha_B = \alpha = 0.05$, $H_0 = 1 \text{ T}$ and $|h_A| = |h_B| = 0.001 \text{ T}$. We have used $M_{A0} = M_{B0} = M_0$ and $M_{A0} = 5M_{B0}$ for AFM and FiM, respectively.
- [34] C. Kittel, *Phys. Rev.* **82**, 565 (1951).
- [35] F. Keffer and C. Kittel, *Phys. Rev.* **85**, 329 (1952).
- [36] A. Kamra, R. E. Troncoso, W. Belzig, and A. Brataas, *Phys. Rev. B* **98**, 184402 (2018).
- [37] F. Schlickeiser, U. Atxitia, S. Wienholdt, D. Hinzke, O. Chubykalo-Fesenko, and U. Nowak, *Phys. Rev. B* **86**, 214416 (2012).